J Electroceram (2008) 20:113–117
DOI 10.1007/s10832-007-9375-0

Preparation and characterization of negative temperature coefficient $(Ni,Mn)_3O_4$–$La(Mn,Ni)O_3$ composite

Chunhua Zhao · Zhongbing Wang · Shouming Wang · Pinghua Yang · Chusheng Chen

Received: 18 May 2007 / Accepted: 22 November 2007 / Published online: 11 December 2007

Abstract The composites made of spinel-structured $(Ni,Mn)_3O_4$ and perovskite-structured $La(Mn,Ni)O_3$ were investigated for potential application as negative temperature coefficient (NTC) thermistor. The composites were prepared using the standard ceramic route. The electrical resistivity of the composite at 25°C was found to decrease by one to two orders of magnitude depending the amount of the low-resistivity perovskite phase, while the thermal constant determining the temperature sensitivity of the NTC thermistor was still reasonably large in the range of 4,000 to 3,000 K, and the resistivity drift after annealing at 150°C for 1,000 h in air was relatively small (~1.2%). The general effective media model was adopted to fit the electrical resistivity data of the composites, giving a value of 0.37 for the percolation volume fraction of the perovskite phase. This work demonstrates that it is possible to tune the electrical resistivity and thermal constant of the spinel-structured oxide through making composite with low-resistivity perovskite-structured oxide.

Keywords NTC thermistors · Composite · Electrical properties · Percolation

C. Zhao · Z. Wang · S. Wang · P. Yang · C. Chen (✉)
Laboratory of Advanced Functional Materials and Devices,
Department of Material Science and Engineering,
University of Science and Technology of China,
Hefei, Anhui 230026, People's Republic of China
e-mail: ccsm@ustc.edu.cn

Z. Wang
School of Chemical Engineering,
Hefei University of Technology,
Hefei, Anhui 230009, People's Republic of China

1 Introduction

Negative temperature coefficient (NTC) ceramic thermistors have been widely used for temperature measurement and compensation due to their high sensitivity to temperature change and low price [1–3]. The specific resistivity ρ of these ceramics follows the well-known Arrhenius relation: $\rho = \rho_0 \exp(E_a/kT)$, where E_a is the activation energy for conduction, ρ_0 the resistivity at infinite temperature, k the Boltzmann's constant and T the absolute temperature. In practice, the NTC thermistors are characterized by two parameters, B, the thermal constant (unit in Kelvin) which is related to $B=E_a/k$, and ρ_{25}, the resistivity at 25°C.

Some applications require NTC materials with a low electrical resistivity while possessing a large thermal constant and a sufficient stability. For spinel-structured manganite, a mostly used NTC material, doping is frequently used to reduce its resistivity. Doping with Cu can reduce the electrical resistivity significantly, but unfortunately at the expense of the stability [4]. And doping with Ni also reduced the electrical resistivity to some extent, but it is difficult to reduce it to ~1,500 Ω·cm [5]. It has been proved very difficult to obtain the required NTC material through doping. Therefore, we propose an alternative approach by introducing a highly conductive component into the spinel oxide. Perovskite-structured $LaMnO_3$ is a good electronic conductor with the electrical resistivity of less than 1 Ω·cm at 25°C [6], and it may not present a serious problem in terms of its compatibility with the spinel manganite. This paper is to report the phase composition, microstructure and electrical properties of the spinel-structured nickel manganite in composite with perovskite-structured lanthanum manganate.

2 Experimental

For preparation of composites $(Ni_{0.75}Mn_{2.25}O_4)_{1-x}(LaMnO_3)_x$ (x=0, 0.1, 0.2, 0.3, 0.4, 0.5), appropriate amounts of $MnC_2O_4{\cdot}nH_2O$, $NiC_2O_4{\cdot}nH_2O$ and La_2O_3 were thoroughly mixed by ball-milling for 24 h in ethanol using ZrO_2 balls, and calcined in air at 850°C for 4 h; the oxalate used was obtained by precipitation of a nitrate solution with oxalic acid at 25°C, and the cation content in the oxalate was determined by the pyrogenation method [7]. The calcined powders were blended with organic binder (PVA, n=1,750, Shanghai Chemical Reagent Co. Ltd., China) and sieved. Disk-shaped powder compacts of diameter 5 mm and thickness 3 mm were formed by uniaxial pressing at 60 MPa followed by isostatic pressing at 300 MPa. The powder compacts were heated in air to 400°C at a rate of 100°C/h and kept at that temperature for 2 h to remove the organic binder, and then heated to 1,150°C at a rate of 150°C/h and maintained at that temperature for 4 h for sintering, and furnace-cooled to room temperature.

The phase composition of the composites was determined by X-ray diffraction (XRD) with Cu Kα radiation (X'Pert Pro, Phillips, Netherlands), lattice parameters were fitted using Powdercell software by the least squares method [8]. The density of the sintered samples was determined by the Archimedes method in Mercury. The microstructure was examined by SEM (JEOL JSM-6700F) coupled with INCA energy dispersive X-ray spectroscopy (EDX); prior to the examination, samples were polished, and thermally etched at 1,100°C in air for 30 min. For electrical resistance measurements, two opposite sides of the sintered disks were polished, coated with platinum paste, heated at 850°C for metallization and then quenched to room temperature. Silver wires were attached as electrode leads. The electrical resistances were measured at 25°C and 50°C by a two-probe technique with an Agilent34401A digital multimeter. The thermal constant B was calculated according to the formula B=3,853.89*ln (R_{25}/R_{50}), in which R_{25} and R_{50} are the resistances at 25 and 50°C, respectively. These samples were aged by heat treatment at 150°C in air for 1,000 h, and the aging is characterized by $\Delta R/R_0=(R-R_0)/R_0$, in which R_0 and R are the resistivity at 25°C before and after the heat treatment.

3 Results and discussion

3.1 Phase composition and microstructure

Figure 1 shows the XRD patterns of $(Ni_{0.75}Mn_{2.25}O_4)_{1-x}(LaMnO_3)_x$ samples with x=0, 0.1, 0.2, 0.3, 0.4, 0.5 and 1.0. Clearly, the composites consist of two phases, cubic spinel-structured oxide (JCPDS: 74-1865) and rhombohedral perovskite-structured oxide (JCPDS: 86-1231). Since element La is much larger in size than other elements Ni and Mn [9], it does not form a spinel-structured oxide; instead, it forms a perovskite-structured oxide with Mn and other transition metal. This is consistent with the EDX analysis showing that La is hardly present in the spinel phase. Composition analysis by EDX also reveals that Ni and Mn are present in both spinel and perovskite phases. Therefore, it is more appropriate to consider the formula $(Ni_{0.75}Mn_{2.25}O_4)_{1-x}(LaMnO_3)_x$ as the nominal composition, and to describe the as-formed composite as the two-phase assembly of $(Mn,Ni)_3O_4$ and $La(Mn,Ni)O_3$. XRD analysis shows that the lattice parameter of the spinel phase increases from 8.401 to 8.433 Å with x increasing from 0.0 to 0.5. It has been also reported that for the single-phase spinel $(Mn,Ni)_3O_4$ sample, higher Mn content corresponds to larger lattice parameter [5]. The observed lattice expansion can be explained in terms of valence and size of the cations occupying the octahedral sites. The Mn-rich spinel is known to possess a cationic distribution $[Mn^{2+}][Ni^{2+}{}_{\alpha}Mn^{3+}{}_{2-2\alpha}Mn^{4+}{}_{\alpha}]O_4$. According to this, when a Ni^{2+} ion is replaced by a Mn^{3+} ion, to maintain the electrical neutrality of the lattice, a Mn^{4+} ion has to convert to Mn^{3+}. In other words, annihilation of one Ni^{2+} ion is accompanied by the annihilation of one Mn^{4+} ion and generation of two Mn^{3+} ions. The sum of these two Mn^{3+}ions in size is larger that that of one Ni^{2+} ion and one Mn^{4+} ion, thus explaining the larger lattice parameter observed for the Mn-rich spinel phase [10]. As to the perovskite phase, its lattice parameters do not vary noticeably with x. It is known that in the perovskite structure both Ni and Mn ions takes the same valence of 3+, and these ions are very close in size [9]. Thus, substitution of Ni by Mn does not result in significant change in the lattice parameters of the perovskite phase.

Figure 2 shows the backscattered SEM images of the composites sintered at 1,150°C. It can be seen that the

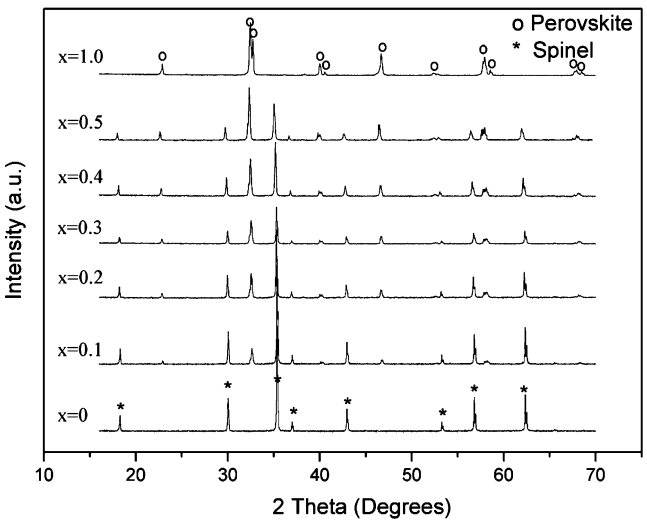

Fig. 1 XRD patterns of $(Ni_{0.75}Mn_{2.25}O_4)_{1-x}(LaMnO_3)_x$

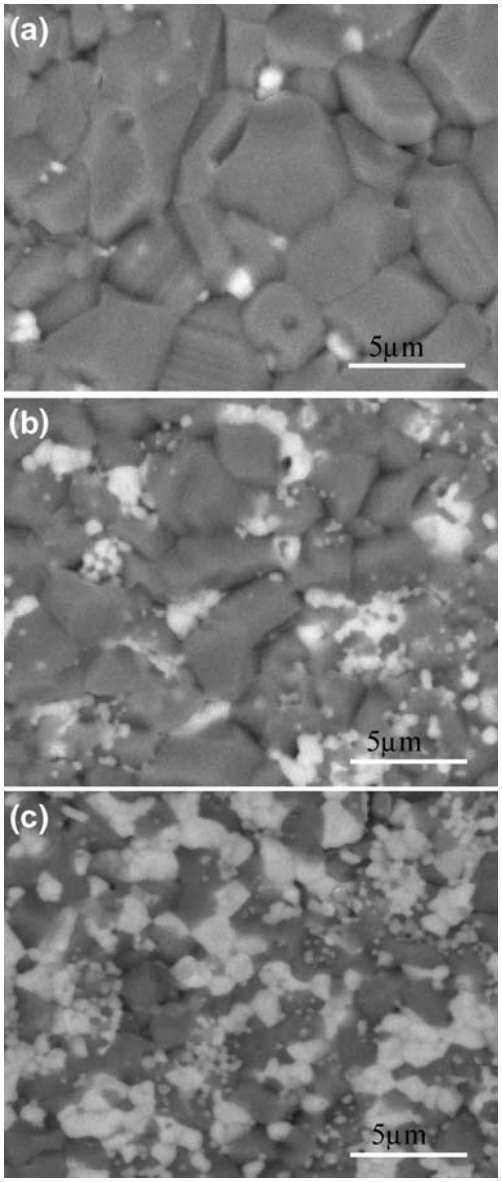

Fig. 2 Backscatter SEM images of $(Ni_{0.75}Mn_{2.25}O_4)_{1-x}(LaMnO_3)_x$ with x=0.1 (**a**), 0.3 (**b**), 0.5 (**c**)

composites consist of two types of grains with different gray level. It is known that La can scatter electrons much more effectively than Mn and Ni, for the atomic number of the former is much higher than those of the latter. Thus, the white grains located at the boundaries of or embedded within the black grains correspond to the perovskite phase, while the black grains the spinel phase. The averaged grain size of the spinel phase decreases from 7.5 to 3.5 μm with x increasing from 0.0 to 0.5. Clearly, the presence of the perovskite phase inhibits the grain growth of the spinel phase. It is also noted that the grain size of the perovskite phase is small compared with the spinel phase. And the grains of the perovskite phase are separated by the spinel phase at low x of 0.1, and become interconnected at higher x of 0.3–0.5.

The as-prepared composites possess a dense microstructure as shown by SEM observation (Fig. 2). The density measurement shows that all the composites prepared have a density over 95% relative the theoretical one. The theoretical density d_{th} is calculated using the formula $d_{th} = \frac{M_p x + M_s(1-x)}{V_p x + V_s(1-x)}$, where x is the molar fraction of the perovskite phase, M the molar weight, V the molar volume, subscripts s and p denote the spinel and perovskite phase respectively. The values for V_s and V_p are calculated using the formulas $V_s = \frac{Na^3}{8}$ and $V_p = \frac{\sqrt{3}Na^2c}{12}$, where a and c are the lattice parameters derived from XRD analysis, N the Avogadro constant. After knowing the values of V_p and V_s, the volume fraction of the perovskite phase f is estimated using the formula $f = V_p^* x \Big/ \left[V_p^* x + V_s^*(1-x)\right] * 100\%$. The results of these calculations are summarized in Table 1.

3.2 Electrical properties

Figure 3 shows the electrical resistivity of the composites at 25°C as a function of the volume fraction f of the perovskite phase. It can be seen that the resistivity decreases gradually with increasing f until f=~0.3; further increase in f leads to a rapid decrease of the resistivity, indicating that the low-resistivity phase (perovskite) has formed a percolative network in the high-resistivity matrix phase (spinel). When f is increased to 0.44, the resistivity is decreased to as low as 18.5 Ω·cm.

The temperature dependence of the electrical resistance was also examined in the temperature range of 25 to 85°C for composites $(Ni_{0.75}Mn_{2.25}O_4)_{1-x}(LaMnO_3)_x$ with x=0–0.5. A linear relationship is observed between Lnρ and the reciprocal of the absolute temperature as shown in Fig. 4. From the temperature dependence, the thermal constant B is calculated. Figure 5 shows B as a function of f. The value of B decreases slowly from 3,937 K to 3,759 K with f increasing from 0 to 0.16, and further increase in f to 0.34

Table 1 The volume fraction of the perovskite phases (f), the theoretical density (d_{th}), measured density (d) and relative density for $(LaMnO_3)_x(Ni_{0.75}Mn_{2.25}O_4)_{1-x}$

X	0	0.10	0.20	0.30	0.40	0.50	1.00
F	0	0.08	0.16	0.25	0.34	0.44	1.00
d_{th}(g/cm^3)	5.19	5.31	5.48	5.60	5.73	5.87	6.84
d(g/cm^3)	4.95	5.05	5.17	5.36	5.49	5.65	6.57
d/d_{th}(%)	95.3	95.1	95.4	95.8	95.7	96.2	96.1

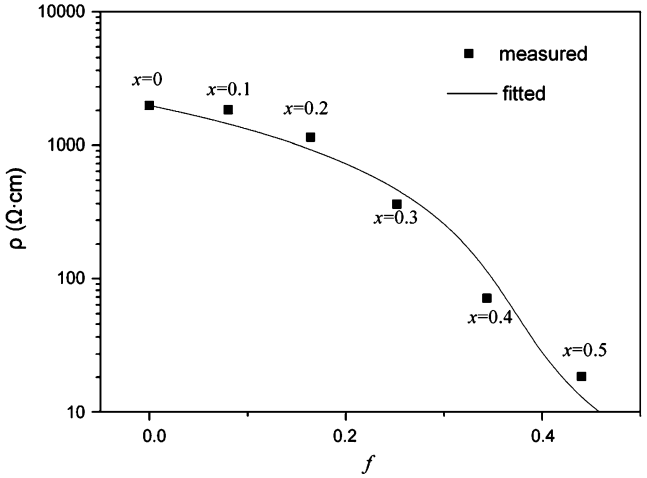

Fig. 3 Measured and fitted electrical resistivity of $(Ni_{0.75}Mn_{2.25}O_4)_{1-x}(LaMnO_3)_x$ as a function of volume fraction of the perovskite phase f

leads to an accelerated decrease of B to 2,150 K. At f of 0.44, B is decreased to 1,700 K, which is close to the value for the single-phase perovskite $LaMnO_3$ (1,500 K).

The composites $(Ni_{0.75}Mn_{2.25}O_4)_{1-x}(LaMnO_3)_x$ with x= 0.1–0.5 also exhibited acceptable stability. It was found that after annealing at 150°C in air for 1,000 h the resistivity at 25°C changed by less than 1.2%, which is slightly smaller than that observed for the single-phase $Ni_{0.75}Mn_{2.25}O_4$ (1.4%).

The transport properties of composite materials including electrical resistivity (conductivity) have been investigated with a variety of percolation models [11]. For a composite made of conductive and insulating materials, it follows from the statistical percolation model that $\sigma = \sigma_0(f - f_c)^n$[12], where σ is the conductivity of the composite, σ_0 and f the conductivity and volume fraction of the conductive component, f_c the critical volume percolation fraction, n the critical exponent for percolation. Unfortunately, this equation cannot be applied to the present composite system, because the spinel phase in the composite does not possesses infinitely large resistivity and thus does not fulfill the condition required by that model. It is also noted that the equation can only be used to describe the electrical conduction in the percolative region ($f>f_c$), but not to the non-percolative region ($f<f_c$). To describe the electrical conduction in a composite containing a low-resistivity phase and a high-resistivity phase in both percolative and non-percolative range, the general effective media model (GEM) [13, 14] has been developed. It follows from GEM model that

$$\frac{(1-f)\left(\rho_H^{1/t}-\rho^{1/t}\right)}{\rho_H^{1/t}+\frac{(1-f_c)}{f_c}\rho^{1/t}}+\frac{f\left(\rho_L^{1/t}-\rho^{1/t}\right)}{\rho_L^{1/t}+\frac{(1-f_c)}{f_c}\rho^{1/t}}=0,$$

where ρ is the resistivity of the composite, ρ_L and ρ_H are the resistivities of the low-resistivity and high-resistivity phase, respectively. For the present composite, the value of ρ_L is taken from a single-phase $LaMnO_3$ sample (0.78 Ω·cm), and the value of ρ_H is obtained from a single-phase sample $Ni_{0.75}Mn_{2.25}O_4$ (1,980 Ω·cm). The measured resistivity of the composite is thus fitted with the GEM equation. In order to make the fitting easier, the GEM equation is transformed to

$$f=\frac{\left(\rho_H^{1/t}-\rho^{1/t}\right)*\left(\rho_L^{1/t}+\frac{(1-f_c)}{f_c}\rho^{1/t}\right)}{\left(\rho_H^{1/t}-\rho^{1/t}\right)*\left(\rho_L^{1/t}+\frac{(1-f_c)}{f_c}\rho^{1/t}\right)-\left(\rho_L^{1/t}-\rho^{1/t}\right)*\left(\rho_H^{1/t}+\frac{(1-f_c)}{f_c}\rho^{1/t}\right)}.$$

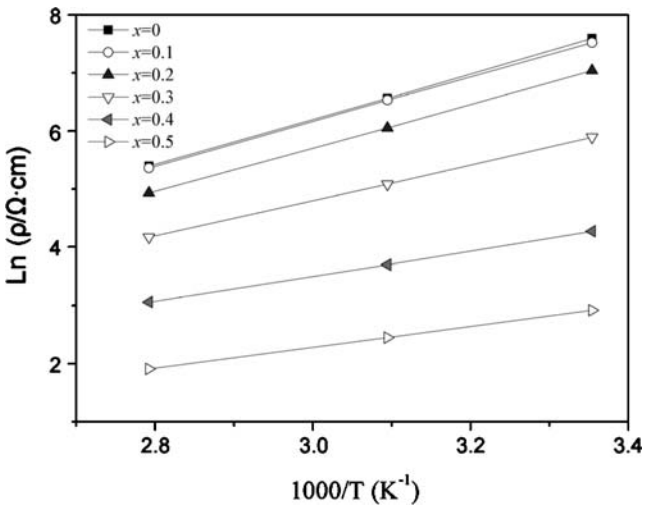

Fig. 4 Arrhenius plot of resistivity for $(Ni_{0.75}Mn_{2.25}O_4)_{1-x}(LaMnO_3)_x$

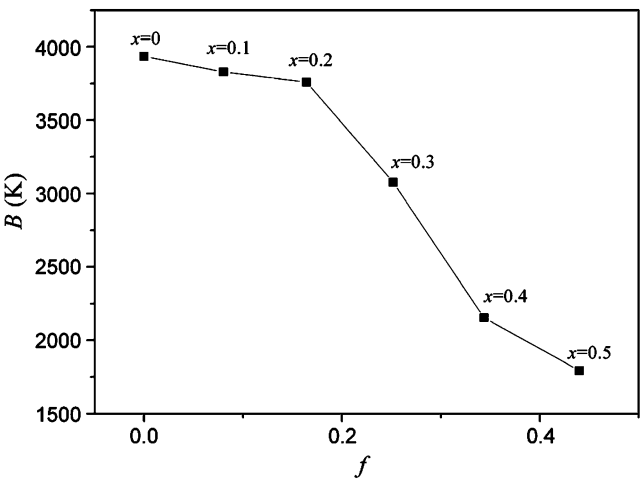

Fig. 5 Thermal constant B of $(Ni_{0.75}Mn_{2.25}O_4)_{1-x}(LaMnO_3)_x$ as a function of volume fraction of the perovskite phase f

The fitting was performed with the help of the commercial software Originpro7.5 using the Levenberg–Marquardt least-squares method [15]. It gives a value of −1.33±0.30 for t and 0.37±0.03 for f_c, indicating that the perovskite phase becomes percolative in the spinel matrix when its volume fraction reaches ~037.

4 Conclusion

Spinel-structured oxide $(Ni,Mn)_3O_4$ in composite with perovskite-structured oxide $La(Mn,Ni)O_3$ has been prepared using the standard ceramic route. The introduction of the low-resistivity perovskite oxide into the spinel oxide yields a composite with reduced electrical resistivity and the desired large thermal constant and acceptable stability. The as-prepared composite is promising for NTC thermistor application.

Acknowledgement This work was supported by National Science Foundation of China (Grant No.: 50225208).

References

1. M.L. Singla, S. Sharma, B. Raj, V.R. Harchekar, Sens. Actuators A **120**, 337(2005)
2. Z.B. Wang, C.H. Zhao, P.H. Yang, A.J.A. Winnubst, C.S. Chen, J. Eur. Ceram. Soc. **26**, 2833(2006)
3. C. Chanel, S. Guillemet-Fritsch, J. Sarrias, A. Rousset, Int. J. Inorg. Mater. **2**, 241(2000)
4. R. Metz, J. Mater. Sci. **35**, 4705(2000)
5. S. Fritsch, J. Sarrias, M. Brieu, J.J. Couderc, J.L. Baudour, E. Snoeck, A. Rousset, Solid State Ionics **109**, 229(1998)
6. I. Maurin, P. Barboux, Y. Lassailly, J.-P. Boilot, F. Villain, P. Dordor, J. Solid State Chem. **160**, 123(2001)
7. X.D. Lou, J. Han, W.F. Chu, X.F. Wang, Q.T. Cheng, Mater. Sci. Eng. B **137**, 268(2007)
8. W. Kraus, G. Nolze, Powder Diffr. **13**, 256(1998)
9. J.A. Dean, Lange's Handbook of Chemistry, 15thst edn. (McGraw-Hill, New York (1999), 4–31
10. S. Guillemet-Fritsch, J.L. Baudour, C. Chanel, F. Bouree, A. Rousset, Solid State Ionics **132**, 63(2000)
11. F. Lux, J. Mater. Sci. **28**, 285(1993)
12. S. Kirkpatrick, Rev. Mod. Phys. **45**, 574(1973)
13. D.S. Mclachlan, J.H. Hwang, T.O. Mason, J. Electroceram. **5**, 37(2000)
14. D.S. McLachlan, Physica A **157**, 188(1989)
15. Origin V75 User's Manual, (Microcal Software Inc., Northampton, MA01060, USA, 2003), p. 514